Molecular Docking Analysis of Human-Cyclooxygenase 1CX2 by 97 Flavonoid Derivatives

Yasodha Krishna Janapati[1], B. Kishore[2], Muralidharan.V[2], Susmitha uppugalla[3],Kasireddy Paul Babu[4], Sumalatha Chepyala[5*]

[1]*School of Pharmacy & Health Sciences, United States International University – Africa P.O. Box 14634 – 00800, Nairobi, Kenya.*

[2]*Department of Pharmaceutical Chemistry, Vishnu institute of Pharmaceutical Education and Research, Vishnupur, Narsapur, Hyderabad, Telangana.*

[3]*Scientist, Quiver Biotech Pvt Ltd, mallapur, hyderabad, 500070, India*

[4]*Department of Pharmacy, St.Mary's College of Pharmaceutical Sciences, Surampalem, East Godavari, Andhra Pradesh,India.*

[5]*Department of Pharmaceutical Chemistry, GeethanjaliCollege of Pharmacy, Cherryal, Keesara, Medchalmalkajgiri District, Telangana-501301, India.*

***Address for correspondence:Sumalatha Chepyala**

sumareddy.chepyala@gmail.com

Abstract: COX (Cyclooxygenase) is the protein that infuses the degradation of PG (prostaglandins) from its substrate, AA (arachidonic acid). The reactions involve 2 steps that area unit 1st step oxidation reaction of AA to hydroperoxy endoperoxide PGG2, go after by 2nd steps future reduction to hydroxyl endoperoxide PGH2. During this work, we tend to study the interaction of ninety-seven flavone derivatives against COX enzymes for anti-inflammatory activity discovery using molecular docking simulation. Docking simulation for every compound was continual molegro virtual docker (MVD) 2013.6.0 for windows was used to predict the degree of each COX binding pockets. Thus, these observations are inconsistent 14 compounds were designated per their best marking values and were designed their hydrogen bonds, electrostatic interactions, steric interactions. However, selective CO-II inhibitors, respectively, N-acetyl-D-glucosamine, protoporphyrin-IX containing Fe, 1-Phenyl-sulfonamide-3-trifluoromethyl-5-parabromophenyl-pyrazole. The remainder of the LIGs is categorized as non-selective inhibitors.

Keywords: Cyclooxygenase, Molegro Virtual Docker, flavonoid

INTRODUCTION

The degradation of prostaglandins from their substrate, arachidonic acid (AA), is catalysed by cyclooxygenases (COX), protein assemblies with HEME enzymes membrane-associated homodimers [1, 2]. There are 2 step in the reactions, and they measure First, AA is converted to the hydroperoxy endoperoxide PGG2 and then, in the subsequent step, is reduced to the hydroxyl endoperoxide PGH2 [1, 2]. Arg120, an amino acid residue used by AA and nonselective NSAIDs that are all carboxylic acids, is not a compulsory site for selective CO-II inhibitors [3, 4]. Vane et al in 1971[5] discovered the apparatus of reticence of COX activity by acetosal and NSAIDs. Although AA is the most common substrate, these enzymes oxygenate other fatty acids with varying degrees of efficiency [6-8].

Bioactive compounds, like diterpenoids and flavonoids (FLD), are tried to point out an anti-inflammatory (AI) activity. While there have previously been many researches on FLDs, in our work we focus on the interaction of 97 flavons with COX enzymes for molecular docking simulation (MDS) and AI discovery. N-acetyl-D-glucosamine, protoporphyrin IX containing Fe, and 1-Phenylsulfonamide-3-trifluoromethyl-5-parabromophenyl-pyrazole was the top moledock score and Plants score (GRID) contenders.

MATERIALS AND METHODS

Protein:

We retrieved the CO-II X-ray crystallographic 3D structures from the online PDB (Protein Data Bank) [(PDB code: 1CX2, resolution $3A^0$complexed with a selective chemical, SC-558, crystallised by Kurumbail et al., 2018) [9]]. The protein was performed exploitation MVD 2013.6.0 tools, the binding modes of CO-II with complexed with a selective inhibitor were studied exploitation ligand (LIG) [10 11]. CO-II binding modalities are shown in Figures 1 and 2, respectively, in a pose view in two dimensions. The volumes of the binding pockets were determined by the plant score and moledock score's exploitation bind module.

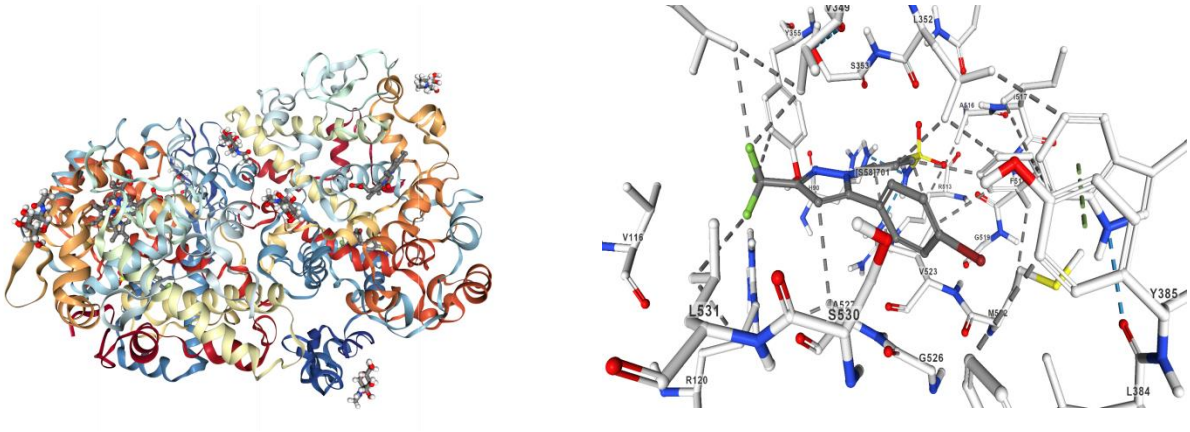

Figure 1: Discovery Studio was used to see the binding pocket of CO-II in green and the binding modes of CO-II [10]

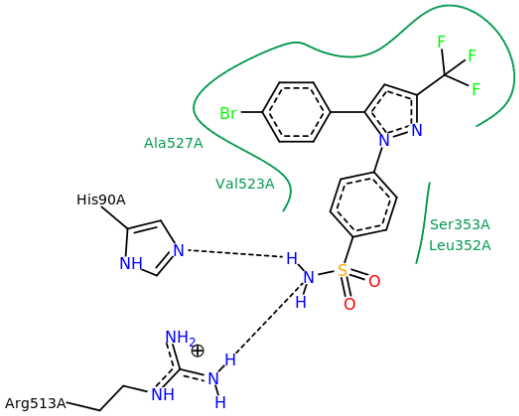

Figure 2: 2D-visualisation of the CO-II binding modes in pose view

Ligand (LIG):

All LIGs were prepared by exploitation chem drawultra 8.0 [12] and were geometry optimized exploitationchem3Dultra 8.0 by using the field of force. The LIGs were saved in pdf file format for additional progression.

Validation of the docking simulation:

Validation was performed redocking of the LIG into its origin location for 10X exploitation windows script command, continuing by conniving the hydrogen bonding, electrostatic and steric interactions. The redocked LIG was then superimposed with the co-crystallized LIG extracted from the protein.

Docking simulation:

Docking simulation for all 16 LIGs was continual 100x exploitation windows script command for MVD 2013.6.0 Tools. Position X = 28.24; Y = -3.24; Z = -6.41 for CO-II (these coordinates area unit at intervals 10 A^0 distance targeted to the LIG position). The binding module in Plants Score [GRID] was used to determine these coordinates. The genetic algorithmic programme parameters for docking conformation to analyse flavones (FLO)s with the highest docking score to the binding mode were established using the default parameters of the automated settings [9, 13]. As a rule, celecoxib was utilised.

Chemical structures: Although these researchers' reports were selected 97 FLOs[14].

1). 5,7-dihydroxy-2-(4-hydroxy-3,5-dimethoxyphenyl)-FLO 7. 5,6,7-trihydroxy-2-phenyl- FLO; 2). 5,7-dihydroxy-2-(3,4-dihydroxyphenyl)- FLO; 3). 5,7-dihydroxy-2-(4-hydroxyphenyl)- FLO; 4) 6,7-dihydroxy-2-(3-hydroxyphenyl)- FLO; 5) 5,7-dihydroxy-2-(4,5 hydroxy-3-(3,4-dihydroxyphenyl)methanone)- FLO; 6) 2-(2,3-dihydro-2-(4-hydroxy-3-methoxyphenyl)-3-(hydroxymethyl)benzo[b][1,4]dioxin-7-yl),5,7-trihydroxy- FLO; 7)5,6,7-trihydroxy-2-phenyl-4H-chromen-4-one; 8)5,7-dihydroxy-2-(3,4-dihydroxyphenyl)-6-methoxy- FLO; 9) 5,7-dihydroxy-2-(4,5hydroxy-3-methoxyphenyl)-FLO; 10) 5,7-dihydroxy-2-(3,4-dihydroxyphenyl)-3-methoxy- FLO; 11) 2-(2,3,4-trihydroxyphenyl)- FLO ; 12)5,7-dihydroxy-8-(1-methylpiperidin-2-yl)-2-phenyl FLO; 13) 5,7-dihydroxy-6-(1-methylpiperidin-2-yl)-2-phenyl FLO; 14).2-(2-chlorophenyl)-5,7-dihydroxy-8-((3R,4S)-3-hydroxy-1-methylpiperidin-4-yl) FLO; 15).5,7-dihydroxy-8-(2-(hydroxymethyl)-1-methylpyrrolidin-3-yl)-2-phenyl-FLO ; 16) 1-(3-chloro-4-(6-ethyl-4-oxo-4H-chromen-2-yl)phenyl)-3-(4-chlorophenyl)urea; 17) 2-phenylpyrano[2,3-e]indol-4(7H)-one; 18) 5-hydroxy-2-(3-hydroxy-4-methoxyphenyl)-3,6,7,8-tetramethoxy- FLO; 19) 2-(3-amino-4-methoxyphenyl)-5-hydroxy-3,6,7,8-tetramethoxy- FLO; 20) 5,6,7,8-tetramethoxy-2-(3,4-dimethoxyphenyl)- FLO; 21) 2-(4-hydroxy-3-methoxyphenyl)-5,6,7,8-tetramethoxy- FLO; 22) 6-chloro-2-(3,5-dimethoxyphenyl)-4H-chromen-4-one; 23) 7-((6-chloropyridin-3-yl)methoxy)-2-(4-((6-chloropyridin-3-yl)methoxy)phenyl)- FLO; 24) 2-(4-bromophenyl)-5,6,7-trimethoxy- FLO; 25) 8-(5-(5,7-dihydroxy-4-oxo-4H-chromen-2-yl)-2-hydroxyphenyl)-5,7-dihydroxy-2-(4-hydroxyphenyl)-4H-chromen-4-one; 26) 5,7-dihydroxy-8-(5,7-dihydroxy-2-(4-hydroxyphenyl)-4-oxochroman-3-yl)-2-(3,4-dihydroxyphenyl)- FLO; 27) 2,2'-([1,1'-biphenyl]-4,4'-diyl)bis(4H-chromen-4-one);28) 2-

(4-(5-(5,7-dihydroxy-4-oxo-4H-chromen-2-yl)-2-hydroxyphenoxy)phenyl)-5,7-dihydroxy-4H-chromen-4-one;29)7-(4-hydroxy-3-methoxyphenyl)-5H-furo[3,2-g] FLO; 30)7-(3,4-dihydroxyphenyl)-5H-furo[3,2-g] FLO; 31)3,4,4a,11b-tetrahydro-2H,10H-pyrano[2',3':4,5]furo[3,2-g]chromen-10-one;32) 2-(3,4-dichlorophenyl)-5-methoxy- FLO; 33) 7,8-dihydroxy-2-phenyl- FLO; 34) 2-(4-(dimethylamino)phenyl)-7,8-dihydroxy- FLO ; 35) 8-(4-(dimethylamino)phenyl) [8,7-d]imidazol-6(1H)-FLO; 36) 2-methyl-8-(4-(pyrrolidin-1-yl)phenyl) [8,7-d]imidazol-6(1H)- FLO; 37) 2-(2-amino-3-methoxyphenyl)-FLO; 38) 2-(2-amino-3-methoxyphenyl)- FLO; 39) 6,7-dimethoxy-2-(4-((pyrrolidin-1-yl)methyl)phenyl)- FLO; 40) 6,7-dimethoxy-2-(3-((pyrrolidin-1-yl)methyl)phenyl)-4H-chromen-4-one; 41) 7-fluoro-2-(4-methoxyphenyl)- FLO; 42) 2-(4-methoxyphenyl)- FLO; 43) 6-chloro-3-hydroxy-2-(2-isopropoxy-4-methylphenyl)- FLO; 44) 2-(3,5-bis(benzyloxy)phenyl)-7-(3-(tert-butylamino)-2-hydroxypropoxy)- FLO ; 45) 7-(2-hydroxy-3-(isopropylamino)propoxy)-2-(3,5-dihydroxyphenyl)-4H-chromen-4-one;
46)5,7-dihydroxy-6-methoxy-8-(4-methylpiperazin-1-yl)-2-(naphthalen-2-yl)- FLO; 47) 6-amino-5,7-dihydroxy-2-phenyl- FLO; 48) 2-(naphthalen-2-yl)- FLO; 49) 2-((5E)-2,4-dioxo-5-((3-(phenyl)methylene)thiazolidin-3-yl)acetyl FLO; 50) 2-((3Z)-2,5-dioxo-3-(2-yl methylene)pyrrolidin-1-yl)acetyl FLO ; 51) 7-hydroxy-2-(4-hydroxyphenyl)-6-(3-methylbut-2-enyl)- FLO; 52) 5-hydroxy-2-(4-hydroxyphenyl)- FLO; 53) 5,7-dihydroxy-2-(3-hydroxy-4-methoxyphenyl)- FLO; 54)3-([1,1'-biphenyl]-4-ylmethyl)-7-hydroxy-2-(4-hydroxyphenyl)-4H-chromen-4-one;55) 5,7-dihydroxy-2-(3-hydroxy-4-methoxyphenyl)-3,6-dimethoxy- FLO; 56) 5-hydroxy -7-yl 4-methylbenzoate FLO; 57) 2-(thiophen-3-yl)-FLO; 58) 5,7-dihydroxy-2-(4-hydroxy-3,5-dimethoxyphenyl)- FLO; 59) 6-methoxy-2-(piperazin-1-yl)- FLO; 60)2,2'-(6,6'-dimethoxy-[1,1'-biphenyl]-3,3'-diyl)bis(5,7-dimethoxy-4H-chromen-4-one);61) 2-(2-chloroquinolin-3-yl)-6-methoxy- FLO; 62) 2-(4-bromophenyl)-6-methoxy- FLO; 63) 5,7-dimethoxy-2-((piperazin-1-yl)methyl)- FLO; 64) 2-(4-fluorophenyl)- FLO; 65) (11E)-1-(2-(4-fluorophenyl)- 4-ylidene)-2-(2,4-dinitrophenyl)hydrazine FLO; 66) 7-(4-(dimethylamino)butoxy)-2-phenyl- FLO; 67) 8-bromo-2-phenyl- FLO ; 68) 6-bromo-2-cyclohexyl- FLO; 69) 5,6,7-trihydroxy-2-(4-hydroxyphenyl)- FLO; 70) 5,7-dihydroxy-2-(4-hydroxyphenyl)-6-methoxy- FLO; 71) 5,7-dihydroxy-2-(2,4-dihydroxyphenyl)- FLO; 72) 6,7,8,9-tetrahydro-5-hydroxy-2-(2,4-dihydroxyphenyl)-8,8-dimethyl-3-(3-methylbut-2-enyl)benzo[g] FLO; 73) 3,5,7-

trihydroxy-2-(4-hydroxyphenyl)-6-(3-methylbut-2-enyl)- FLO; 74) 3,5,6,7,8-pentamethoxy-2-(3,4-dimethoxyphenyl)- FLO; 75)6-(5-(5,7-dihydroxy-4-oxo-4H-chromen-2-yl)-2-hydroxyphenyl)-5,7-dihydroxy-2-(4-hydroxyphenyl)-4H-chromen-4-one;76) 6-amino-3-methoxy-2-(2-methoxyphenyl)- FLO; 77) N-(2-(2-fluorophenyl)-3-methoxy-6-yl)acetamide FLO; 78) 5-methoxy-8-(4-methoxyphenyl)-2,2-dimethyl-2H,6H-pyrano[3,2-g]chromen-6-one; 79) 3,5,6,7-tetrahydroxy-2-(3,4-dihydroxyphenyl)- FLO ; 80) 6-amino-2-(2-fluorophenyl)-3-methoxy- FLO; 81) 6-amino-3-methoxy-2-(4-methoxyphenyl)- FLO; 82) 6-amino-2-(4-(trifluoromethyl)phenyl)-3-methoxy- FLO; 83) 2-(3,5-di-tert-butyl-4-hydroxyphenyl)-7-hydroxy- FLO; 84) 7-(2-hydroxy-3-(propylamino)propoxy)-2-phenyl- FLO; 85) 2-(benzo[d][1,3]dioxol-6-yl)-3,5,6,7,8-pentamethoxy- FLO; 86) 2-(piperidin-1-yl)ethyl 3-methyl -8-carboxylate FLO; 87) 2-(benzo[d][1,3]dioxol-6-yl)-7-hydroxy- FLO; 88) 2-(3-bromophenyl)-5,7-dihydroxy-8-(3-methylbut-2-enyl)- FLO; 89) 5,7-dihydroxy-2-(3,4,5-trimethoxyphenyl)-8-(3-methylbut-2-enyl)- FLO 90. 5,7-dihydroxy-2-(3-hydroxyphenyl)-8-(3-methylbut-2-enyl)- FLO; 90) 5,7-dihydroxy-2-(3-hydroxyphenyl)-8-(3-methylbut-2-en-1-yl)-4H-chromen-4-one; 91) N-(3-(4-(2-methoxyphenyl)piperazin-1-yl)propyl)-3-methyl-4-oxo-2-phenyl-8-carboxamide FLO;92) 7,8-dihydroxy-2-phenyl- FLO; 93) 4-oxo-2-(3-((E)-2-(quinolin-2-yl)vinyl)phenyl) -8-carboxyl FLO; 94) 5-hydroxy-2-(3-hydroxy-4-methoxyphenyl)-3,6,7,8-tetramethoxy-FLO; 95) 4-oxo-2-(4-((E)-2-(quinolin-2-yl)vinyl)phenyl)-carboxyl FLO; 96)(E)-4-oxo-2-(4-(2-(quinolin-2-yl)vinyl)phenyl)-4H-chromene-8-carboxylic acid; 97) 5,6-dimethoxy-2-(4,5-dimethoxybenzo[d][1,3]dioxol-6-yl)- FLO. General structure of FLO (Figure 3).

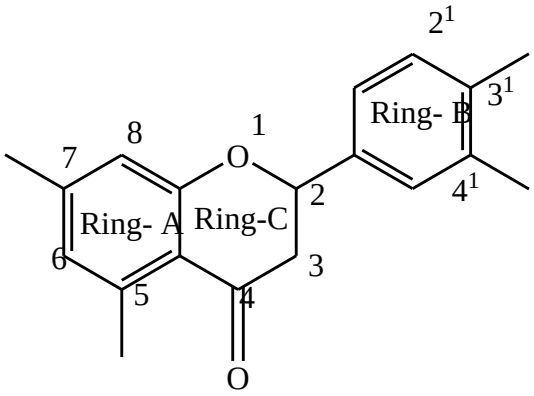

Figure 3: General structure of FLOs

S.No	2D-Chemical Structure	S.No	2D-Chemical Structure	S.No	2D-Chemical Structure
1	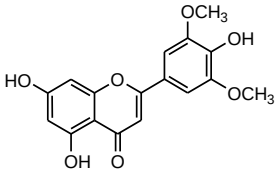	2	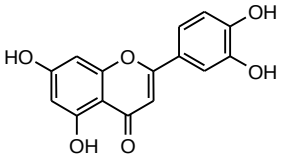	3	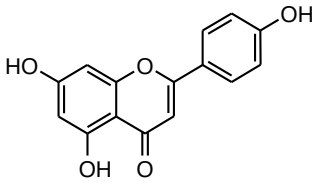
4	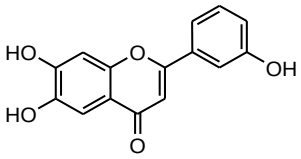	5	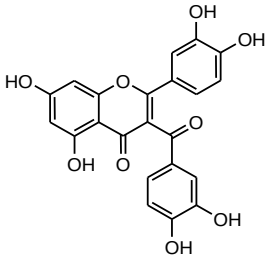	6	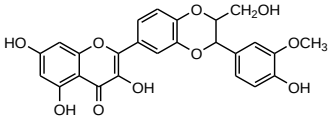
7	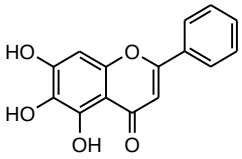	8	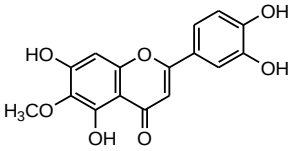	9	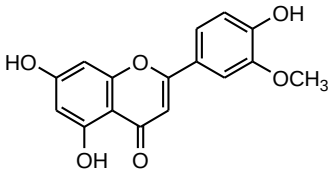
10	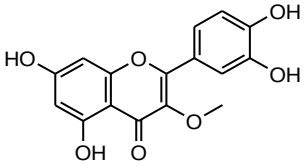	11	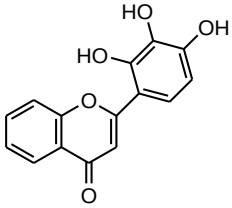	12	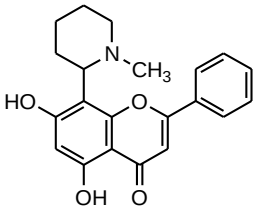
13	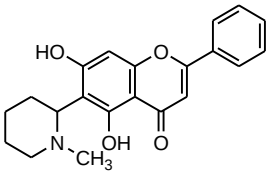	14	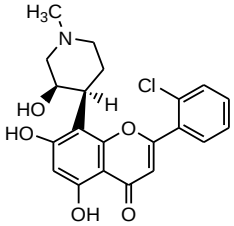	15	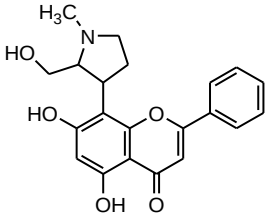
16	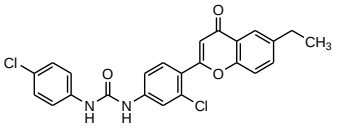	17	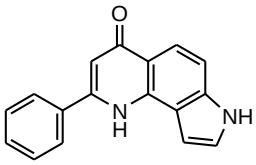	18	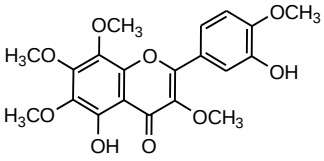
19	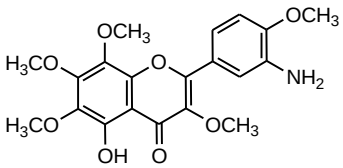	20	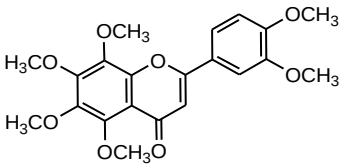	21	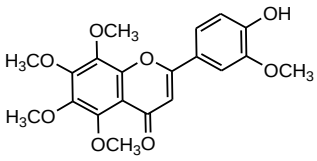

22

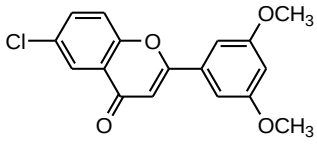

23

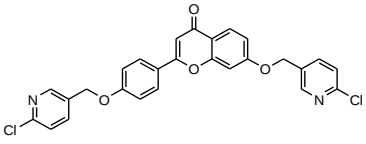

24

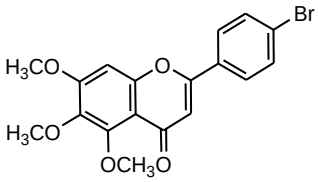

25

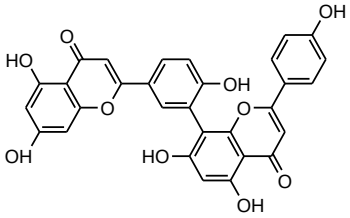

26

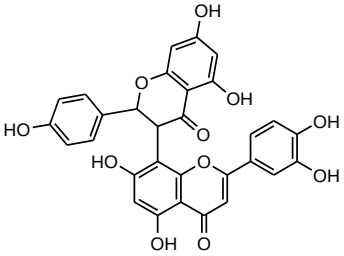

27

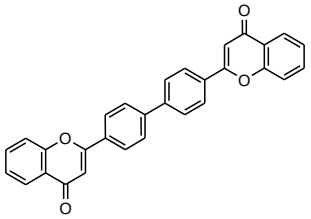

28

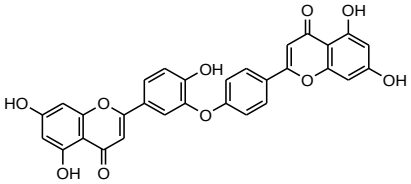

29

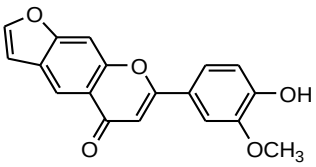

30

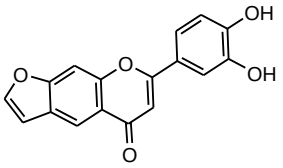

31

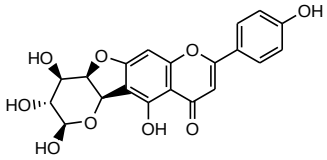

32

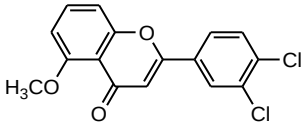

33

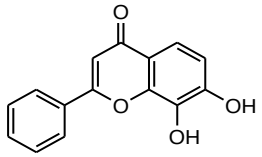

34

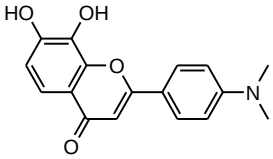

35

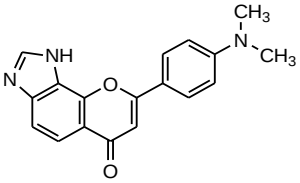

36

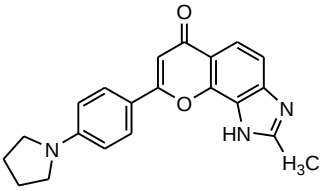

37

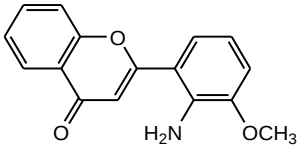

38

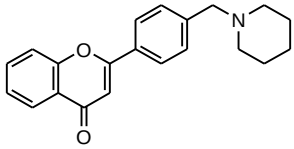

39

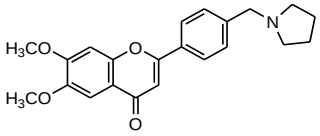

40

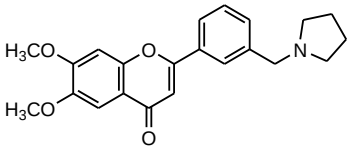

41

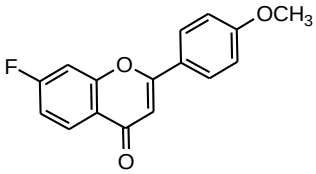

42

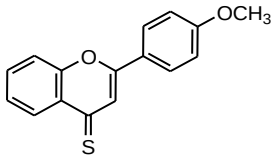

43

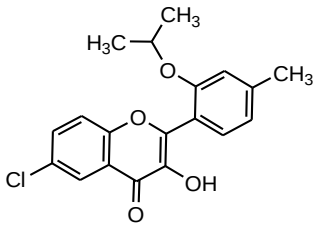

44

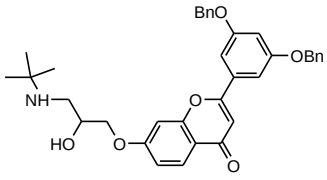

45

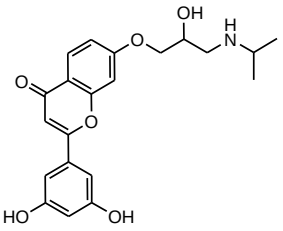

46

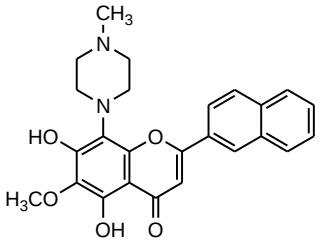

47

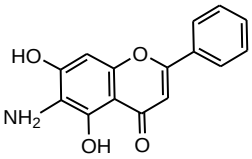

48

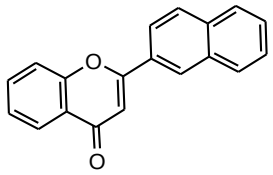

49

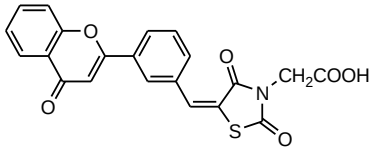

50

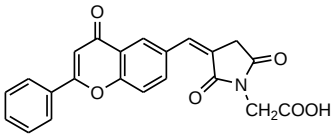

51

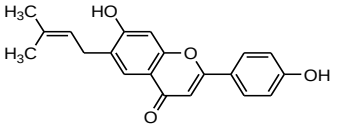

52

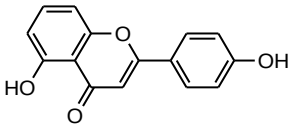

53

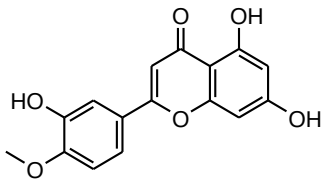

54

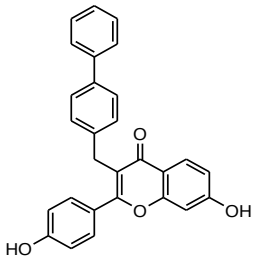

55

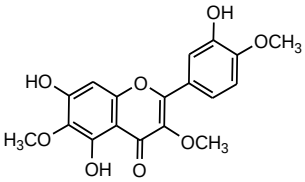

56

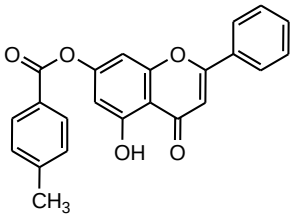

57

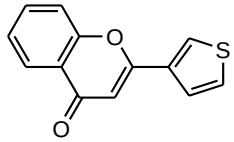

58

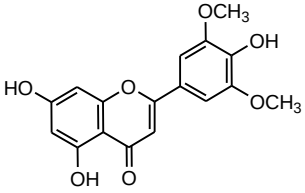

59

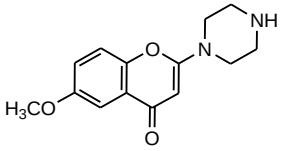

60

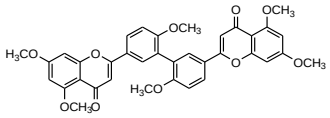

61

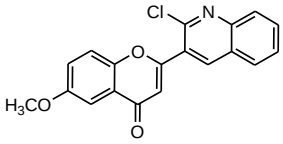

62

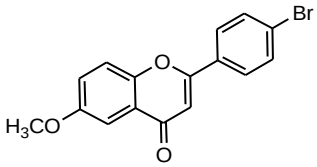

63

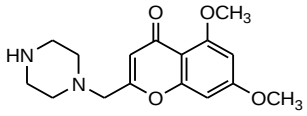

64

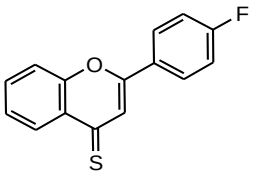

65

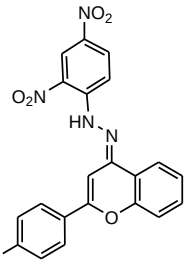

66

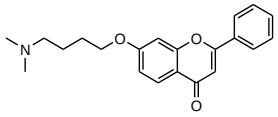

67

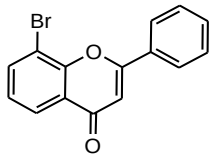

68

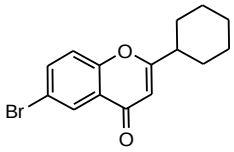

69

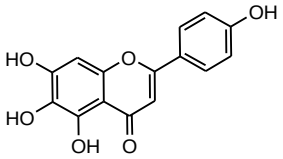

70

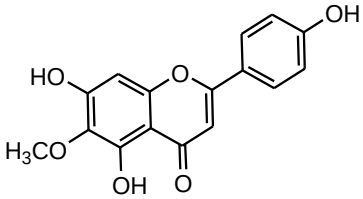

71

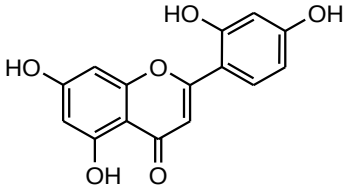

72

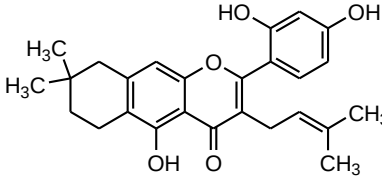

73

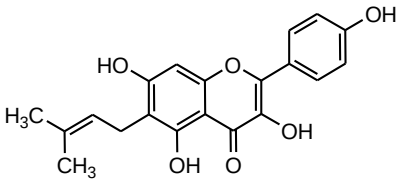

74

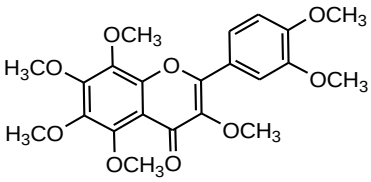

75

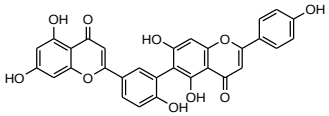

76

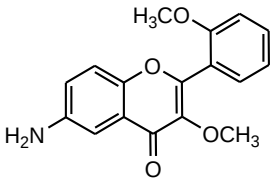

77

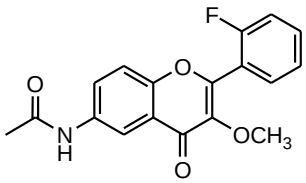

78

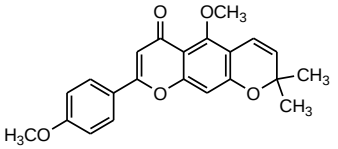

79

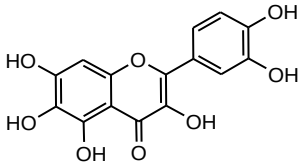

80

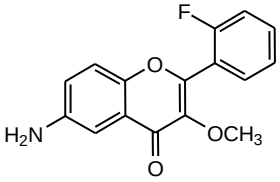

81

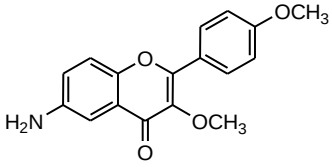

82

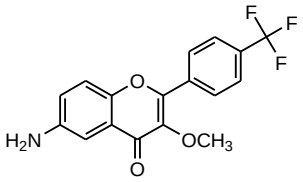

83

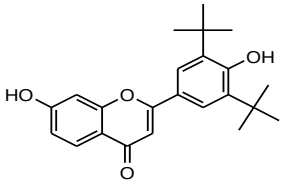

84

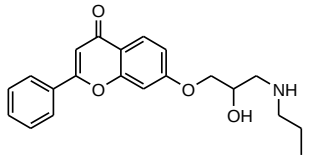

85

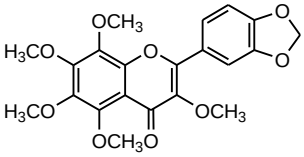

86

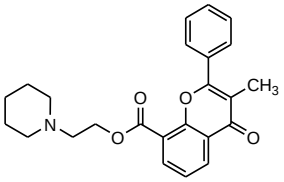

87

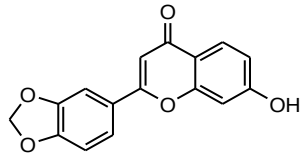

88

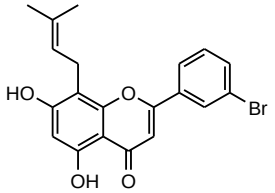

89

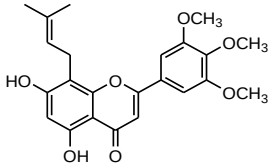

90

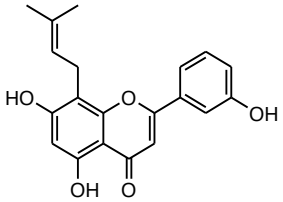

91

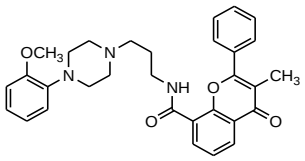

92

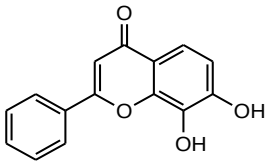

93

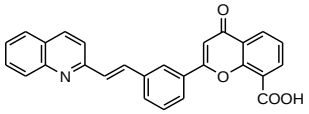

94

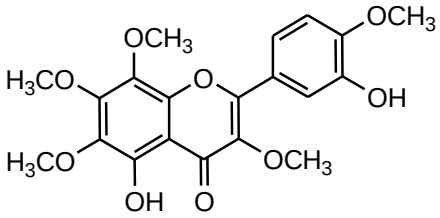

95

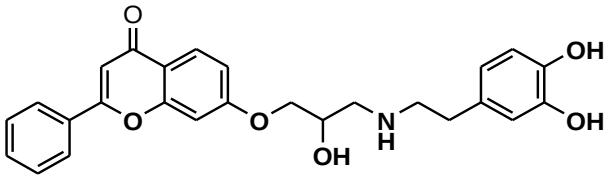

96

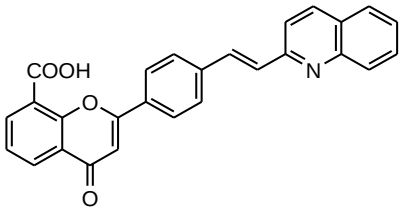

97

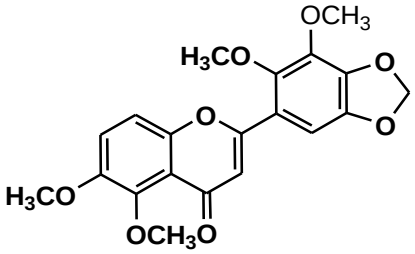

RESULT AND DISCUSSION

All compounds were assessed using MVD 2013.6.0 MD experiments to examine the possibility of COX inhibitory characteristics of the selected drugs. First, using the bind module in plants score, the binding pocket volume of CO-II was estimated. The findings are displayed in table 1.

Table 1: Top Docking Score molecules

S. No	Name of compound	MDS (k.cal/mol)	Re-rank scores (k.cal/mol)	Hydrogen bonding (k.cal/mol)
1	LIG	-85.0216	-75.9266	-8.65832
2	celecoxib	-116.994	-93.5236	-4.9489
3	Compound 27	-196.235	-164.25	-0.326616
4	Compound 16	-161.485	-125.153	-3.70113
5	Compound 79	-116.796	-103.341	-16.8383
6	Compound 96	-173.867	-110.221	-0.108599
7	Compound 76	-172.761	-99.6216	-9.31129
8	Compound 04	-129.205	-85.7346	-15.862
9	Compound 05	-133.185	29.1664	-12.8889
10	Compound 56	-131.818	-100.764	-11.1953
11	Compound 6	-99.7595	-83.8723	-10.955
12	Compound 54	-118.494	-71.9772	-10.6441
13	Compound 97	-155.76	-135.889	-3.64552

14	Compound 57	-158.488	-134.571	0
15	Compound 74	-151.045	-129.746	-7.90601
16	Compound 37	-153.231	-129.58	-1.51902

During LIG preparation progression, all chosen compounds were designed and arithmetic optimized. Thus, these observations square measure scheming hydrogen bonds, electrostatic and steric interactions. Amino acid residues in the COX site of CO-II, these docking data is by following per under-reported information on cycloprodigiosin reported by the researcher Kurumbail, R.*et al* (2018), wherever where amino acid residues such as Glu 67, Ser 138, His 226, Gln 270, Gln 284, Phe 292, His 365, Glu 398, Pro 514, Lys 573, His 278, Val 287, Cys 575, Val 582, Asn 144, Pro 280, Phe 422, Pro 547, Thr 212, Glu 290, Gln 400, Gln 429, Pro277, Val 228 associated with A chain of CO-II protein were involved for protein-LIG complementary activity.

In this study, we tend to additional examined and compared the structure-function relationships of the reticence of CO-II (PG synthase-2) complexed with a selective inhibitor, SC-558 in complex with an inhibitor with a total of 97 FLDs by measurement N-acetyl-D-glucosamine,1-Phenylsulfonamide-3-trifluoromethyl-5-parabromoph enyl-pyrazole, HEM for the previous three enzymes respectively, for the last two enzymes. The FLDs employed were FLO, nine hydroxylated FLOs, four methoxylated FLOs, eight hydroxylated methoxyFLOs, 4′,5,7-trihydroxyisoFLO, and 4′-methoxy-5,7-dihydroxyFLO. FLO, 4′,5,7-trihydroxylFLO, and its glycoside were also used. These FLDs' spectral interactions with five P_{450} were investigated, and their inhibitory potencies against-558 in the complex was compared. Additionally presented and assessed are MD studies of the interactions of these FLDs with the active sites of several cyclooxygenase-2 enzymes.

MD studies were performed on 97 selected FLDs with CO-II enzymes using the reported crystal structures of SC-558. The 97 FLDs examined were top-five ranked active poses (viz LIGs, Moldock score, Reranks of poses, H- bonds) total of 14 FLO compounds,

Based on the outcomes of the LIG's interaction with the CO-II enzyme, the amino acid residues in the substrate recognition site (SRS) are highlighted. The aligned amino acid residues of LIG-based on the amino acid sequence of N-Acetyl-D-Glucosamine, 1-

Phenylsulfonamide-3-Trifluoromethyl-5-Parabromoph Enylpyrazole, and HEM additionally indicated in Figure-4, respectively. N-Acetyl-D-Glucosamine, 1-Phenylsulfonamide-3-Trifluoromethyl-5-Parabromoph Enylpyrazole molecules were encircled by amino acid residues Ser-38 and Asn-68, which are reported to be key amino acids within the interaction of aligned with the LIG.

Celecoxib is standard, bounded by amino acid residues were Val 165, Asp 499, Pro 474, Lys 468, Asn 39, Ser 462, Glu 465, Gln 461, Ser 38 associated with A-chain of LIGFigure-5.

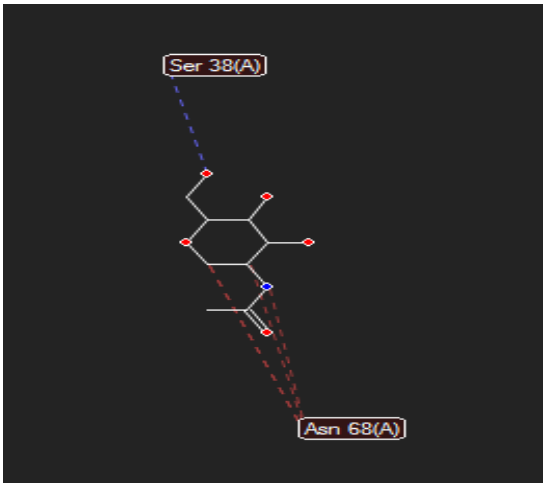

Figure 4: MDS of LIG

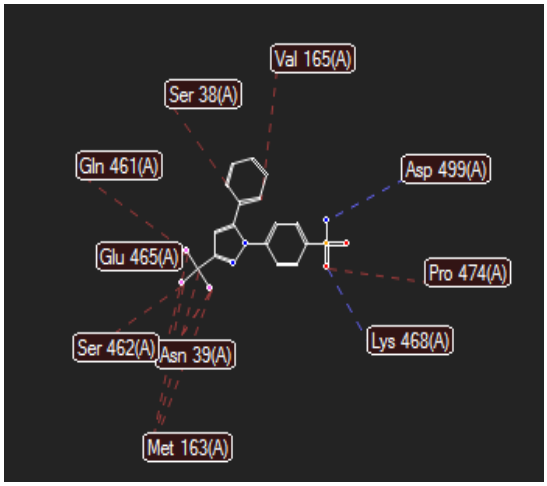

Figure 5: MDS of Celecoxib

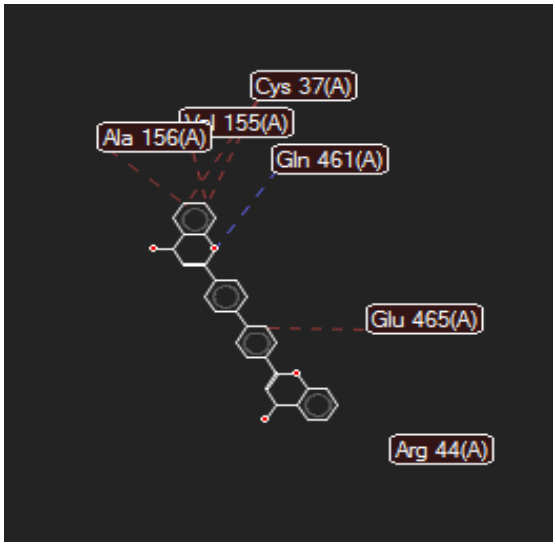

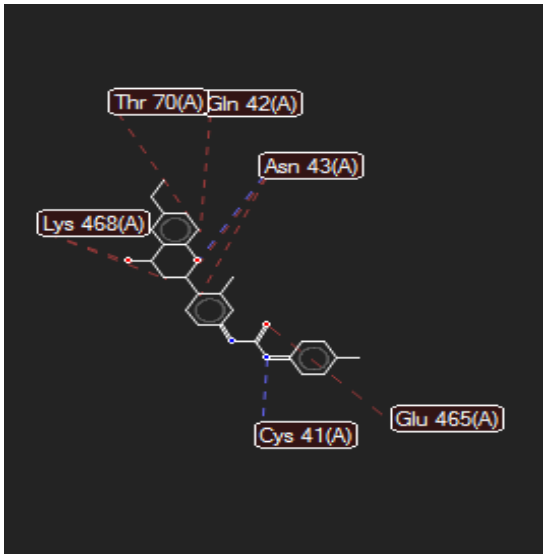

Figure 6: MDS of Compound 27 **Figure 7: MDS of Compound 16**

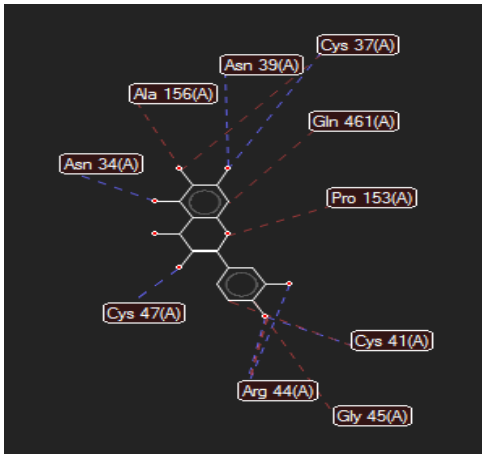

Figure 8: MDS of Compound 79

Compounds 16 and 27 of the FLO family were docked into the LIG, and the findings demonstrated that (Figures 6 and 7) the former two FLDs provided equivalent orientations in interacting with the LIG's CO-II enzyme. In these former five cases, the B ring (Figure-3) of the FLD compounds was placed near the active site of the LIG, and the FLD molecules were surrounded by amino acid residues Cys-41, Glu-465, Asn-43, Gln-42, Thr-70, Lys-468 in UNIX 16 and Arg-44, Glu-465, Gln-561, Val-155, Cys-37and Al-156 in UNIX27 which have been disclosed to be key amino acids in the interaction with LIG.

Compound-79, a FLO, was docked into the LIG, and the results revealed that it interacted with the Cyclooxygenase 2 enzyme in the LIG in comparable ways to the previous two FLDs (Figure -8). The FLD molecules were enclosed by the amino acid residues Arg-44, Gly-45, Cys-41, Pro-153, Gln-461, Cys-37, Asn-39, Ala-156, Asn-34, and Cys-47 in compound79, which have been reported to be important amino acids in the interaction with LIG, in the first five of these cases.

CONCLUSION

We concluded that various mechanisms by which FLDs inhibit COX-II in human (PG-2) when it is complexes with a selective inhibitor and LIG, and that these reticence mechanisms vary depending on the enzymes and inhibitors. Surprisingly, the being there of diphenolic (compound-16, 27) groups was observed to boost the efficacy of

reticence against these LIG enzymes. It was discovered that a portion of the 5, 7-dihydroxyl group in the FLO's ring-A increased the compound-79's ability to block these LIG enzymes. According to MD studies, the six FLDs and the five LIG enzymes interact in various directions.

Ethical Approval

No

REFERENCES:

I. Smith WL, Garavito RM, DeWitt DL. Prostaglandin endoperoxide H synthases (cyclooxygenases)-1 and− 2. Journal of Biological Chemistry. 1996;271(52):33157-60.

II. Simmons DL, Botting RM, Hla T. Cyclooxygenase isozymes: the biology of prostaglandin synthesis and reticence. Pharmacological reviews. 2004 September 1;56(3):387-437.

III. Kurumbail RG, Kiefer JR, Marnett LJ. Cyclooxygenase enzymes: catalysis and reticence. Current opinion in structural biology. 2001 December 1;11(6):752-60.

IV. Bakhle YS. Structure of COX-1 and CO-II enzymes and their interaction with inhibitors. Drugs today. 1999;35(4-5):237-50.

V. Vane JR. Reticence of prostaglandin synthesis as a mechanism of action for aspirin-like drugs. Nature new biology. 1971;231(25):232.

VI. Vecchio AJ, Simmons DM, Malkowski MG. Structural basis of fatty acid substrate binding to cyclooxygenase-2. Journal of Biological Chemistry. 2010;285(29):22152-63.

VII. Dilber SP, Dobric SL, Juranic ZD, Markovic BD, Vladimirov SM, Juranic IO. Docking Studies and Anti-inflammatory Activity of β-Hydroxy-β-arylpropanoic Acids. Molecules. 2008;13(3):603-15.

VIII. Vane JR, Botting RM. Mechanism of action of anti-inflammatory drugs: an overview. In Selective CO-II Inhibitors.Springer Dordrecht, 1998; 1-17.

IX. Sunil Junapudi, Sindura Gollamudi.The Molecular Docking of Selected Antiretroviral Agents and Chloroquine Derivatives as COVID-19 Inhibitor N3 (6LU7) using Molegro Virtual Docker.I nventi Rapid: Molecular Modeling.2021; 2021(3):1-6.

X. https://www.rcsb.org/structure/1CX2

XI. http://www.rcsb.org/pdb/explore/litView.do?structureId=1CX2.

XII. www.cambridgesoft.com.

XIII. Mason RP, Walter MF, McNulty HP, Lockwood SF, Byun J, Day CA, Jacob RF. Rofecoxib increases susceptibility of human LDL and membrane lipids to oxidative damage: a mechanism of cardiotoxicity. Journal of Cardiovascular Pharmacology. 2006;47:S7-14.

XIV. Singh M, Kaur M, Silakari O. FLOs: An important scaffold for medicinal chemistry. (EJMC) European journal of medicinal chemistry . 2014;84:206-39.